Journal of Thermal Analysis and Calorimetry
https://doi.org/10.1007/s10973-024-13199-0

Self-nucleation (SN) and successive self-nucleation and annealing (SSA) as powerful tools to determine the composition of polyolefin post-consumer recycled blends

Sebastián Coba-Daza[1,4] · Andreas Albrecht[4] · Dario Cavallo[3] · Davide Tranchida[4] · Alejandro J. Müller[1,2]

Received: 6 December 2023 / Accepted: 6 April 2024

Abstract

For the incorporation of post-consumer recycled (PCR) resins in mechanical recycling processes, it is crucial to determine their composition accurately. The blends of linear low-density polyethylene (LLDPE) and low-density polyethylene (LDPE) in PCR film resins pose a challenge due to their varying ratios. This study introduces a quantitative method that employs the successive self-nucleation and annealing (SSA) technique to analyze commercial PCR LLDPE/LDPE blend compositions. Our method is an efficient way to assess these blend compositions, offering an improved analysis compared with traditional methods. We established a series of calibration curves based on the SSA final melting trace to validate our approach. The SSA technique's efficacy was compared with the robust NMR method, showing that SSA can predict LLDPE contents in the blends with comparable accuracy. We demonstrate that the SSA methodology is an accurate and reliable technique for assessing complex waste streams, thereby facilitating the optimization of recycling processes and advancing the goals of sustainable materials management.

Keywords Recycled blends · Thermal fractionation · Successive self-nucleation and annealing · LLDPE/LDPE ratio quantification

Introduction

Recent research and global decisions have led to the development of advanced techniques and practical solutions to address the global concern of plastic waste and the reuse of these valuable resources. Many companies and organizations have taken action to address sustainability and embrace the circular economy by investing resources to remove plastics from waste streams. To achieve a circular economy in the plastics industry, effective collection of plastic waste [1, 2], improved sorting techniques [3, 4], and sustainable product design are necessary [5]. The main approaches are chemical and mechanical recycling, individually or combined [6]. Chemical recycling involves breaking down used polymers into their building blocks or restoring them to a purified state as new feedstock materials [7]. On the other hand, mechanical recycling is a cost-efficient approach involving incorporating recycled polymers and virgin polymers into new products at different ratios [8]. In various applications, such as film materials, blends of low-density polyethylene (LDPE) and linear low-density polyethylene (LLDPE) are

✉ Dario Cavallo
dario.cavallo@unige.it

✉ Davide Tranchida
davide.Tranchida@borealisgroup.com

✉ Alejandro J. Müller
alejandrojesus.muller@ehu.es

[1] POLYMAT and Department of Polymers and Advanced Materials: Physics, Chemistry and Technology, Faculty of Chemistry, University of the Basque Country UPV/EHU, Paseo Manuel de Lardizabal, 3, 20018 Donostia-San Sebastián, Spain

[2] Basque Foundation for Science, IKERBASQUE, Plaza Euskadi 5, 48009 Bilbao, Spain

[3] Department of Chemistry and Industrial Chemistry, University of Genova, via Dodecaneso 31, Genoa 16146, Italy

[4] Borealis Polyolefine GmbH, Innovation Headquarters, St. Peterstrasse 25, 4021 Linz, Austria

Published online: 11 May 2024

commonly used, which is why the use of recycled materials in such applications is desired.

LDPE and LLDPE resins are commonly combined to improve film processing over different applications [9, 10]. LDPE long-chain branching (LCB) enhances melt strength and offers a high degree of shear-thinning, improving extrudability and flowability [11]. On the other hand, LLDPE is a widely used material in flexible packaging with a density range of 0.915–0.935 g/cm^3 [11]. It is produced through catalytic copolymerization of alpha-olefins like 1-butene, 1-hexene, and 1-octene with ethylene [11]. Incorporating LLDPE in such blends reduces density and increases tie chains, forming amorphous rubbery domains [12]. These amorphous domains bridge the adjacent crystalline lamellar regions, enhancing the film's large deformation properties, such as impact, tear, and stretchability [13, 14].

Commercially available post-consumer recycled (PCR) materials may contain LLDPE, LDPE, and polypropylene (PP) resulting from mixed films in the recycling stream [15]. PP might be present in small quantities due to contamination. Identifying and determining the composition of these PCR blends is crucial for targeted applications [12]. The composition of LLDPE/LDPE blends can be determined by analyzing the inherent differences in melting and crystallization characteristics between LDPE and LLDPE during polymer crystallization, either from a molten or solution state [16–19]. The density of LLDPE and LDPE strongly affects their thermal properties, mainly due to branching content (and chain length) and how chain branches are distributed among polymer chains [12]. Secondarily, the average molecular weight (Mw) and molecular weight distribution (MWD) also play a role. Blends of LDPE and Ziegler–Natta LLDPE (ZN-LLDPE) are phase-segregated in the crystalline state when analyzed using DSC experiments [16]. LLDPE tends to crystallize from its molten state at higher temperatures, and linear crystallizable sequences of similar lengths may be able to co-crystallize in blends with LDPE [20]. To quantify the composition of the LLDPE/LDPE blend, relative peak sizes (peak height or area) can be used to estimate the blend's composition. Prasad [18] proposed a technique that uses DSC heating scans to evaluate the LDPE content in a neat ZN-LLDPE/LDPE blend. Calibration curves were generated using known C4-LLDPE/LDPE, C6-LLDPE/LDPE, and C8-LLDPE/LDPE blends, with the α-olefin type identified using Fourier transform infrared (FTIR) spectroscopy before quantification [18]. However, this method is challenging in estimating LDPE/LLDPE content in post-consumer and post-industrial recycled materials since identifying the comonomer type through FTIR is difficult due to contamination [12]. Furthermore, in PCR materials, the presence of multiple comonomers makes the proposed DSC method impractical for quantifying the PCR blend composition, but it is suitable for comparison purposes.

Other methodologies have been developed to investigate the quantification of LLDPE and LDPE in different blends. Recent research introduced a technique based on nuclear magnetic resonance (NMR) to determine the composition of LLDPE/LDPE blends [21]. This method involves comparing the ^{13}C NMR spectra of the blend with those of neat LDPE, using integrated peak areas derived from specific resonance peaks present in both LDPE and blended samples. By quantifying the total integrated area of specific spectral regions within the LLDPE/LDPE blend and then comparing it to the corresponding LDPE measurements, an estimation of the average mass percentage of LDPE in the blend can be obtained [21]. However, the accuracy of this approach critically relies on having a reference LDPE sample with a closely matched density and processing characteristics, which poses a significant challenge when dealing with mixed post-consumer and post-industrial recycled materials [21]. In addition, implementing this methodology requires excluding specific outlier data points from the analysis to achieve an acceptable level of variance. This data filtering process may impact the accuracy of the estimated LDPE content [21].

In a recent investigation, Hashemnejad [12] proposed a composition analysis of virgin and post-consumer recycled LLDPE and LDPE blends. A crystallization elution fractionation (CEF) technique was proposed for accurate composition analysis. Calibration curves for CEF were fabricated using blended LLDPE and LDPE resins, showing consistent trends. Fourier transform infrared spectroscopy and nuclear magnetic resonance were used to identify comonomer types in LLDPE. In this case, they report that CEF and DSC techniques offer similar LDPE content results for virgin polymer blends, depending on density. However, CEF proves more precise and reliable for estimating LDPE content in PCR LLDPE/LDPE blends, particularly those potentially containing inorganic compounds [12].

In the present investigation, self-nucleation (SN) and self-nucleation and annealing (SSA) protocol employing differential scanning calorimetry (DSC) were used to determine the LDPE/LLDPE composition and quantify PP contamination within commercially post-consumer recyclates. The methodology enables the fractionation of the materials during the thermal treatment, separating such fractions by temperature ranges and then associating the different fractions with the corresponding fractions in neat materials. Calibration curves are constructed using model blends, mimicking the recyclates' composition, and the evaluation of LDPE/LLDPE content is addressed by selecting the appropriate temperature range from the resulting melting trace from the SSA protocol. When quantifying PP content, the self-nucleation protocol is used in *Domain III*. In this case, unmolten crystals present during the thermal protocol act as nucleating agents to boost PP crystallization and enhance its

melting enthalpy. This enables an approximated quantification of the PP content in the post-consumer recycled materials. The results can be compared with the nuclear magnetic resonance (NMR) technique.

Experimental

Different resins of linear low-density polyethylene (LLDPE), low-density polyethylene (LDPE), and polypropylene (PP) were selected for the fabrication of the model blends. Borealis Polyolefine GmbH kindly provided them. The polymer's density and Melt Flow Index (MFI) are listed in Table 1. The selected LLDPE grades covered the density range typically found in recycled PE streams. Melt blending was used to prepare model PP/LLDPE/LDPE and LDPE/LLDPE blends in a microcompounder Xplore MC15HT at 190 °C, 50 rpm, and 2-min residence time, with applied nitrogen to prevent degradation. Based on previous experiments, melt blending conditions were chosen adequately to achieve homogenization while preventing polymer degradation. The model blend formulation is composed of two groups. The first one encompasses the model blends with PP, denoted as MODEL_PP-X, where X stands for the amount of PP incorporated in the blend as 1, 3, 5, and 7%, the remaining composition is equal amounts of LLDPE and LDPE, for example, MODEL_PP-1 is composed of 1% PP, 49.5% LLDPE, and 49.5% LDPE. The second group of model blends is denoted as, for instance, MODEL_LDPE + LLDPE-Y, where Y indicates LLDPE density. For each LLDPE density, three compositions were fabricated (LDPE/LLDPE 30/70, 40/60, and 50/50) for the creation of the calibration curves. LLDPE and LDPE components are listed in Table 1. For a further indication of the blend's name and specific composition, refer to Table S1 in the supplementary information. In addition, six different materials from post-industrial waste (denoted as REC_0 to REC_5) were selected to evaluate the proposed method's effectiveness in estimating PP and LDPE/LLDPE content via self-nucleation and self-nucleation and annealing (SSA) methodology.

Table 1 Materials used to prepare model blends along with their density and MFR

Material	Density/kg m^{-3}	MFR (190 °C/2.16 kg)
LLDPE_918	918	1.5 g/10 min
LLDPE_923	923	0.25 g/10 min
LLDPE_931	931	0.2 g/10 min
LLDPE_935	935	15 g/10 min
LDPE	920	0.25 g/10 min
PP	920	2.8 g/10 min

The thermal properties of neat LLDPE and LDPE, along with their model blends, were studied using a TA Instruments DSC (model 2500), calibrated with indium, zinc, and tin under a nitrogen atmosphere. Film sheets were prepared from the samples, and circular sections were loaded into a standard DSC pan. The samples from the first group of model blends (MODEL_PP-X) were heated from room temperature to 200 °C at 10 °C min^{-1} and kept for 3 min at that temperature to remove the thermal history. Immediately, the blends were cooled to 0 °C and then heated to 200 °C at 10 °C min^{-1}. The estimation of PP, in this case, is based on the obtained endotherms from the second heating step.

As for the second group of model blends (PE model blends), the samples were heated from room temperature to 180 °C at 10 °C min^{-1} and kept at 180 °C for 3 min to remove any thermal history. Afterward, the materials were cooled at 10 °C min^{-1} to 0 °C, followed by a second heating step at 10 °C min^{-1} until 180 °C. Quantitative analysis was based on the observed endotherms during this second heating step.

To estimate the PP content in model and recycled blends, the adopted self-nucleation (SN) protocol is based on the method devised initially by Fillon et al. [22], with subsequent reviews by Michell et al. [23] and Sangroniz et al. [24]. The process consists of six sequential steps conducted at a controlled heating rate of 10 °C min^{-1}. The steps applied are as follows: In Steps 1 and 2, thermal history was removed by heating the material well above its melting temperature (typically 30 °C above the melting peak) and then cooling it down at a fixed rate of 10 °C min^{-1} to establish a "standard" thermal history. Step 3 consists of heating the sample to a specified temperature, T_s. Step 4 is a 5-min thermal treatment at the chosen T_s. The selection of these T_s might result in different possible outcomes: *Domain I* when the temperature is high enough for complete melting, *Domain II* when a lower temperature is chosen, facilitating partial or complete melting, which promotes self-seeding or melt memory, respectively, and finally, *Domain III* with a temperature low enough that results in the annealing of the unmolten crystals at T_s. In step 5, the sample is cooled from T_s to room temperature, and its crystallization temperature is monitored. Finally, in step 6, a final heating run identifies changes in the material's melting temperature due to the self-nucleation treatment, revealing the actual *Domain* based on the T_s selection.

This self-nucleation temperature program addressed the different domains in MODEL_PP-X blends. As already mentioned above, in *Domain III,* the unmolten crystals boost the epitaxial crystallization of the PP phase. Therefore, in the last heating, step 6, it is possible to quantify the enthalpy associated with the self-nucleated PP, which gives a good approximation to the content of PP in the sample. This was used to estimate the PP content of the

recycled materials and the model PP materials to compare the accuracy of the prediction. In all experiments, the values of specific parameters in the SN protocols were kept constant: heating and cooling rates at 10 °C min^{-1}, a thermal treatment time at T_s of 5 min, the initial temperature of 200 °C for crystalline-memory erasure, and a final temperature of 20 °C at the end of the cooling step. These specific scan rates and annealing time values were chosen based on previous self-nucleation studies [25–28]. As part of this investigation, the only variable that changed in each experiment was the value of T_s.

As for the determination of LDPE/LLDPE content in model and recycled materials, the successive self-nucleation and annealing (SSA) protocol was employed. The temperature program utilized for the SSA fractionation was developed by Müller et al. [25, 29, 30]. More details are given in the Supplementary Information (Figures S1 and S2). In brief, this protocol starts with steps resembling the previously mentioned standard SN protocol. In this case, steps 1 to 4 of the SN were repeated, where the first T_s will be the $T_{s,ideal}$ of the material. $T_{s,ideal}$ is the temperature leading to the highest nucleation density without annealing of un-molten crystals, i.e., the minimum T_s temperature in *Domain II*. This temperature corresponds to the lowest temperature within *Domain II*. Consequently, each material will fractionate from the same initial ideally self-nucleated condition. For comparison purposes, $T_{s,ideal}$ of recycled materials (i.e., $T_{sideal} = 128$ °C) was evaluated in all the samples. It is essential to mention that subjecting the material to 5-min thermal conditioning at the first *Ts* value does not cause annealing. No thermal fraction is produced since this T_s value lies within *Domain II*. The subsequent steps are crucial as they determine sample fractionation. After step 4, a cooling ramp is applied to 20 °C, followed by heating to T_{s2}, which is 5 °C lower than the initial T_s. This process is repeated by decreasing T_s by 5 °C (i.e., 5 °C fractionation window) in each step until 11 fractions are created (12 selected temperatures).

Results and discussion

Determination of polypropylene content as contamination in recycled blends.

The quantification of polyolefin blend components has been reported extensively using various methodologies [17, 18, 21, 31–35]. One of the main techniques depends on the crystallinity obtained from the melting enthalpy in the standard heating–cooling–heating thermal protocol using DSC equipment. This methodology consists of determining the area under the curve for the specific blended material in the adequate temperature range and comparing it with the neat polymer enthalpy value. In this way, it is possible to estimate the composition of the material [33] roughly. However, the accuracy of using enthalpy to determine polymer crystallinity from DSC measurements has been questioned because they are obtained under non-equilibrium conditions [17, 31]. In addition, the melting transitions are influenced by sample crystallinity, and the thermal history of samples could also impact the analysis, potentially limiting the technique's accuracy for quantitative determinations [36]. Nevertheless, this technique is commonly used for its simplicity and easiness in quality control laboratories as the first approach to qualitative characterization. It is essential to mention that PP has melting temperatures (Tm) that are different from LLDPE and LDPE, resulting in different transition peaks in the DSC scans and allowing their proper identification [35].

A conventional DSC protocol (heating–cooling–heating) was initially employed to determine PP composition in recycled blends. The resulting second heating endotherms from the standard protocol in the recycled

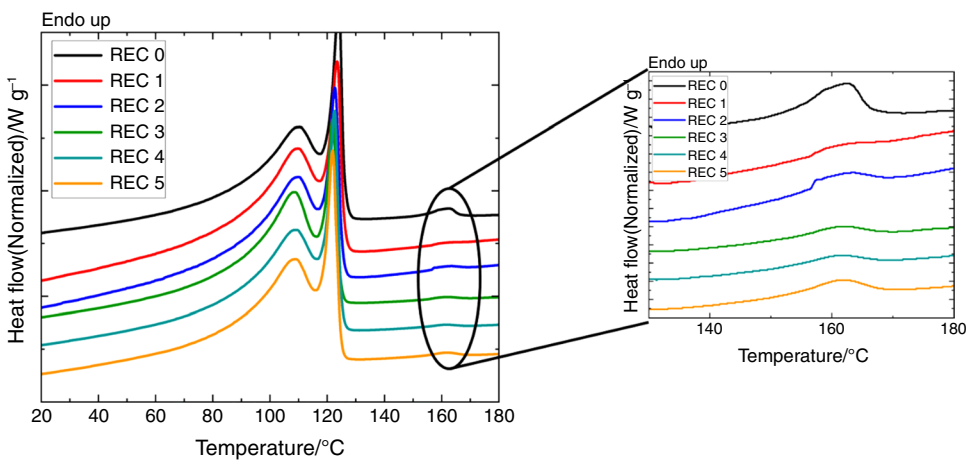

Fig. 1 DSC second heating scans of the post-consumer recycled blends

materials are shown in Fig. 1. The recycled materials possess three different melting peaks assigned to different components in the blend. Starting from the low temperatures, the first peaks located at around ~ 110 °C are associated mainly with LDPE, while those at higher temperatures, such as around ~ 123 °C, are due to LLDPE. These thermal melting transitions agree with those reported in the literature [37]. However, it is crucial to highlight that, as recognized in the literature, the crystallization behaviors of LLDPE and LDPE frequently involve co-crystallization [38]. These intricate interactions depend on variables such as the specific fabrication method (involving catalysts like Ziegler–Natta types) and the inherent comonomer composition within LLDPE. It is important to note that due to these complex interplays, the resulting crystalline peaks have the potential to overlap during the DSC standard measurements [39]. In addition, at much higher temperatures (~ 160 °C), a small melting transition appears. At this temperature, the peak is associated with the PP component, as the melting temperature coincides with the melting temperature for PP and incidentally is much higher than the equilibrium melting temperature of PE. In this case, the content of PP is low, as indicated by the small peak height and area; therefore, it is associated with contamination in the PE recycled material. This contamination is because the sorting step is not 100% efficient during recycling, allowing slight material contamination [40]. Quantifying the PP content to propose applications to the final recycled material and quality control assurance is crucial.

As mentioned before, to address the quantification of crystalline polymer materials with standard DSC, the method is based on the comparison between the enthalpy of melting (ΔH_m) from the obtained DSC scans in both virgin and blended material. This method allows the composition calculation, which is then used here to compare further with the SSA and NMR methodologies. Table 2 presents the obtained results from the PP estimation via DSC.

Table 2 Comparison of PP quantification in recycled materials with different techniques

PP estimation/%				
Sample	Standard DSC	Standard self-nucleation in *Domain II*	Self-nucleation (SN) (*Domain III*)	NMR
REC_0	2.00	2.49	3.10	5.00
REC_1	0.38	0.42	0.51	1.09
REC_2	0.86	1.09	1.12	1.89
REC_3	0.62	0.83	0.92	1.55
REC_4	0.57	0.79	0.87	1.30
REC_5	0.94	1.07	1.35	2.29

In addition, the different recycled materials were studied using the self-nucleation methodology to obtain the different thermal characteristics of the components in the blend and its distinctive domains and quantify the PP content. The different self-nucleation domains for the PP phase within the recycled blends were successfully obtained by applying a range of selected self-nucleation temperatures (T_s). In *Domain I*, a lack of change in the crystallization temperature of the PP phase indicates the complete melting of crystals, as evident from the red curves in Fig. 2. In addition, in *Domain II*, a noticeable increase in the PP crystallization temperature (T_c) was observed during cooling scans originating from the selected T_s, as shown in the blue curves in Fig. 2A. This change is due to self-nucleation, which significantly increases the density of nucleation sites. Consequently, an increase in the crystallization temperature is obtained [41]. Finally, an annealing peak appeared in Domain III at temperatures higher than the primary fusion endotherm, highlighted by the green curves in Fig. 2B. The distinctive high-temperature peak that emerged initially at $T_s = 165$ °C is attributed to the annealing of un-molten crystals.

When the T_s value reaches 160 °C, annealing affects a large population of the existing PP crystals, producing a sharp melting endotherm well separated from the PE melting endotherms. The obtained endotherm at $T_s = 160$ °C is then used to estimate the PP composition more accurately than the untreated DSC standard melting scan. Furthermore, the observation of these self-nucleation *Domains* is extended to other recycled materials, confirming their consistent occurrence and enabling the methodology to estimate the PP content and compare it with the DSC standard method and with the self-nucleation in *Domain II*.

An interesting additional observation emerged when examining the influence of self-nucleated PP on the PE phase. As the crystallization temperature increased in the PP phase, a corresponding increase occurred in the PE phase crystallization temperature. This trend aligns with our earlier studies in different model systems [27, 28, 42–45], and it is extended here to real recycled materials, as illustrated in Figures S3 and S4. Since the selected T_s value is high enough to melt the PE phase completely, the PP phase acts as a nucleating agent for the LLDPE, increasing its crystallization temperature.

Table 2 presents the polypropylene content prediction in post-consumer recycled materials using the standard and the self-nucleation methods. Additionally, the quantification results from NMR are provided for comparative analysis. Notably, the conventional DSC protocol underestimates the polypropylene composition compared to the NMR measurements. In addition, the self-nucleation (SN) protocol demonstrates closer alignment with the calculated NMR values. Consequently, the self-nucleation method emerges as a resourceful and time-effective alternative to the conventional

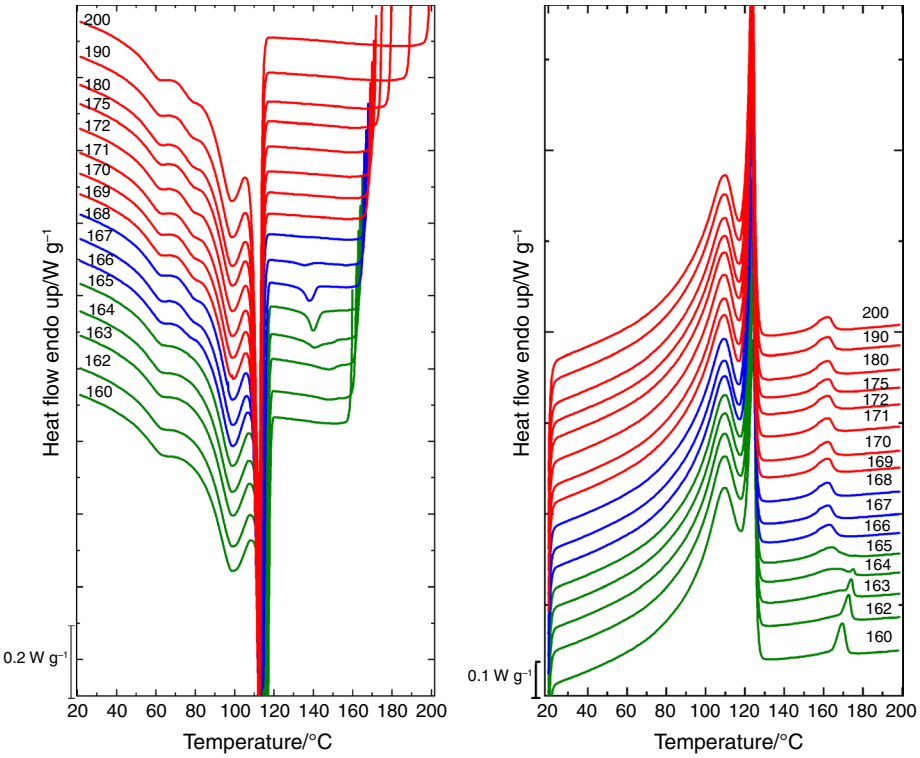

Fig. 2 DSC scans for the recycled material REC_0: (**a**) cooling and (**b**) subsequent heating after treatment at T_s. Domains are color-coded: red for Domain I, blue for Domain II, and green for Domain III

Table 3 Obtained values of $T_{s,\ ideal}$ from the application of the self-nucleation protocol (SN)

Sample	$T_{s,ideal}$/°C
LLDPE_918	123
LLDPE_923	126
LLDPE_931	128
LLDPE_935	128
MODEL_LDPE/LLDPE_918 (70/30; 60/40; 50/50)	123
MODEL_LDPE/LLDPE_923 (70/30; 60/40; 50/50)	126
MODEL_LDPE/LLDPE_931 (70/30; 60/40; 50/50)	128
MODEL_LDPE/LLDPE_935 (70/30; 60/40; 50/50)	128
REC0 to REC5	128

standard protocol, thus showcasing its potential for application in environments where time is of the essence, e.g., quality control procedures as an initial step for quantification.

Quantification of LDPE/LLDPE in recycled blends

The SSA thermal fractionation protocol was applied according to the recommendations by Muller et al. [26, 29, 30] to analyze the behavior of each material individually. Before that, the selection of the $T_{s\ ideal}$ was performed. Using the SN protocol specifically for the PE component of model and recycled materials, the $T_{s,\ ideal}$ values were obtained and are given in Table 3.

The correct application of the SSA protocol demands the use of the $T_{s,\ ideal,}$ as a starting point because this is the temperature that causes maximum self-nucleation (maximum increase in T_c) without producing annealing, as the sample is ideally self-nucleated; it contains the maximum possible nucleation density [26]. This is necessary when the results of the SSA method will be used to quantitatively determine short-chain branching distribution data through suitable calibration curves obtained by FTIR and NMR. Nevertheless, in this case, the comparison at different $T_{s,ideal}$ temperatures would be difficult since the melting peak distribution and the areas under the different melting peaks will be different.

As suggested in the literature [26, 27], in recycled materials, the selection of a common highest $T_{s,\ ideal}$ for all materials under study, is a convenient way to compare a series of samples using the same thermal fractionation procedure. Together with a constant fractionation window (5 °C) and the same thermal history, the tree parameters make the SSA results fully comparable. For this reason, a $T_s = 128$ °C was selected as the highest value; therefore, all the SSA procedures were carried out at this T_s. When selecting a constant T_s for performing SSA in different materials, the resulting melting curve will match all valley positions, thus making the comparison easier. To fractionate the individual components, the standard SSA protocol was used with the selected constant T_s and incorporating 12 steps (128, 123, 118, 113, 108 °C; 103 °C; 98 °C; 93 °C; 88 °C; 83 °C; 78 °C; and 73 °C).

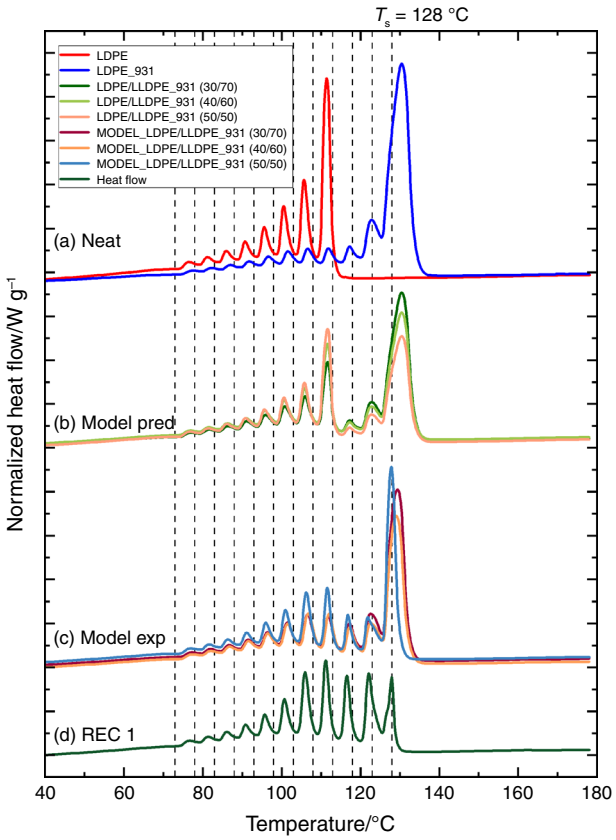

Fig. 3 Final DSC heating scan after applying the SSA thermal protocol to: (**a**) neat LDPE and LLDPE, (**b**) the sum of neat curves at different compositions to create the model predicted, (**c**) the experimental model blends at different compositions, and d) the resulting DSC scan from recycled material number 1

The final heating curves after the SSA protocol for neat, model, and recycled materials at a specific density are shown in Fig. 3. The sum of the neat DSC traces at different compositions producing theoretically predicted curves is also represented. We will denote these traces as "unmixed blends," as they are a simple weighted superposition of the neat polymers' experimental DSC plots [25]. The SSA curve obtained for neat LDPE shows only eight melting peaks because no annealing was produced at the highest T_s temperature since $T_s = 128$ °C is within *Domain II*, where no annealing occurs. Regarding the LLDPE, the characteristic melting peaks of the produced fractions were obtained. For each LLDPE density, the corresponding SSA is presented in Figures S5–S7 in the supplementary information. The unmixed blends, in this case, were generated by adding each neat material's corresponding DSC trace normalized by the selected composition; for instance, when generating the unmixed LDPE_LLDPE_931 (70/30) curve, the neat LDPE curve was multiplied by its corresponding fraction (0.7). Then, it was summed with the corresponding fraction of the LLDPE curve (0.3). In this way, the specific contributions of different compositions were obtained. This is the theoretical curve one would obtain if there were no interactions between the components, i.e., the unmixed blend.

Nonetheless, as it is generally known [46], the different types of polyethylenes can have different interactions, such as co-crystallization or dilution of the higher-temperature crystallizable phase. Therefore, experimentally, the obtained fractionated SSA curves will differ from the unmixed blends when such interactions arise. The unmixed blend curves in this context are meaningful since they provide insights into which theoretical thermal fractions differ from the experimental curve.

Three different unmixed blends were constructed per each selected LLDPE. Figure 3 also presents the model experimental blends (these are blends made with virgin materials, not recycled ones), and in this case, the density of 931 kg m^{-3} is shown as an example. The first observation that can be made from the experimental curves of the model blends is that they differ from the unmixed blends. This means the peaks do not follow the same pattern as in the unmixed blends but instead have a characteristic behavior. When the first three high-temperature peaks from unmixed and model blends curves are compared, it is observed that the melting peaks corresponding to the model blends fractions are narrower and that the melting temperature varies among the peaks. As previously noted, this distinct behavior is attributed to the co-crystallization effect of the different polyethylene chains in the model blends.

Typically, polyethylene blends, which have a similar melting range and are miscible in the melt, often undergo co-crystallization between specific chain populations where the methylene sequence length (MSL) is of comparable length [25]. In fact, this co-crystallization can be observed during the second heating scan in a standard heating–cooling–heating thermal protocol in DSC, as presented in Fig. 4. In this case, it comes together using the already mentioned SN and SSA protocol to avoid most of the co-crystallization effects obtained in standard DSC for the LLDPE composition estimation.

We now turn to the design of calibration curves obtained from the model blend that can correlate areas under specific thermal fractions and the quantity of LLDPE in the blends. The evaluation was conducted using the TRIOS software in the following manner: Initially, the total area was derived from the SSA melting curves for each material. The temperature limits for integration were set and consistently applied across all model and recycled blends to guarantee precise comparisons. Specifically, the selected temperature range covered from 25 to 140 °C. Next, the area under each thermal fraction within the final SSA heating run was determined. It is crucial to note that the integration limits chosen for each fraction remained consistent across all materials.

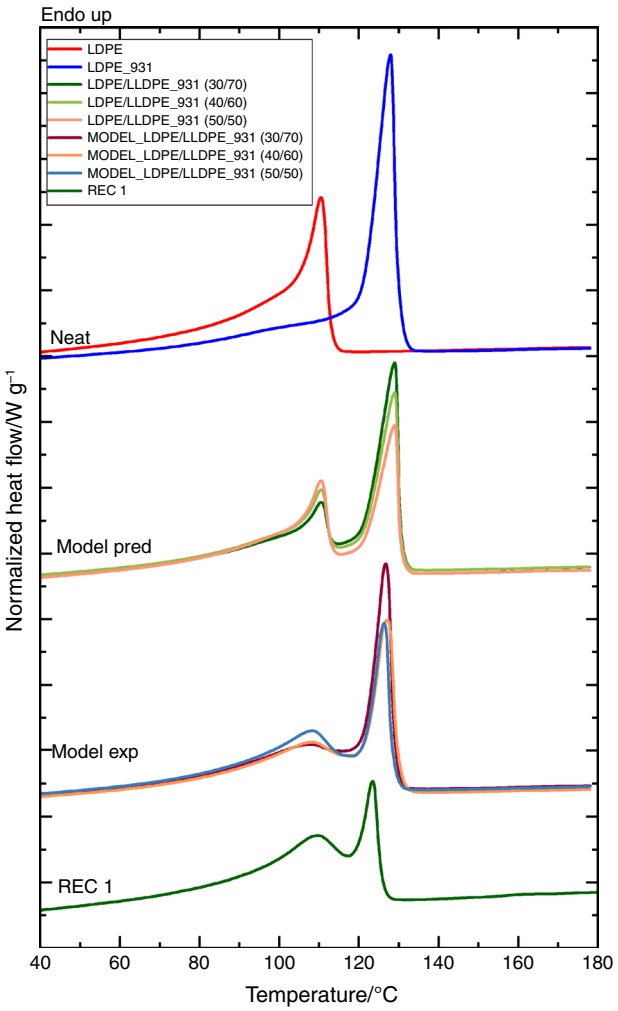

Fig. 4 DSC second heating scans of neat, model predicted, model experimental, and recycled material number 1, showing the effects of co-crystallization

Given that the fractionation window and the selected seeding temperature (T_s) were identical, the valleys in each fraction appeared at precisely the same values, corresponding to the applied T_s temperatures. Details regarding the integration limits for every analyzed peak can be found in Table S2 in the supplementary information. For a more accurate representation, the area of the first two and three peaks (counting from high to low temperatures; the first peak always corresponds to the melting of the highest temperature thermal fraction) was normalized against the total melting area. This step of normalization was undertaken to remove any potential sources of variation. Two sets of calibration curves were subsequently established. The first set centered on the combined normalized area of the initial two high-temperature peaks, spanning a temperature range from 140 to 119.7 °C. Four distinct calibrations were derived, each corresponding to the different LLDPE densities used (see Fig. 5A). For the second set of calibration curves, the temperature range was extended from 140 to 114.9 °C to include the first three high-temperature fractions (see Fig. 5B).

A linear trend is observed in the calibration curves. Specifically, higher-density materials display a higher normalized value from the sum of the initial peaks, while in the lower-density LLDPEs, a lower value is observed. Given that LLDPE at lower densities typically has a higher branching content, as a result of the SSA protocol, fractionation at lower temperatures is greater because of the high branching content, implying that the corresponding peaks at these temperatures will possess a larger area. Since the calibration curve evaluation involves normalizing all peaks, an increase in the total area relative to the first two or three peaks results in a reduced normalized value. In contrast, for higher-density LLDPE, which has a lower short-chain branch content and exhibits, on average, longer linear chain

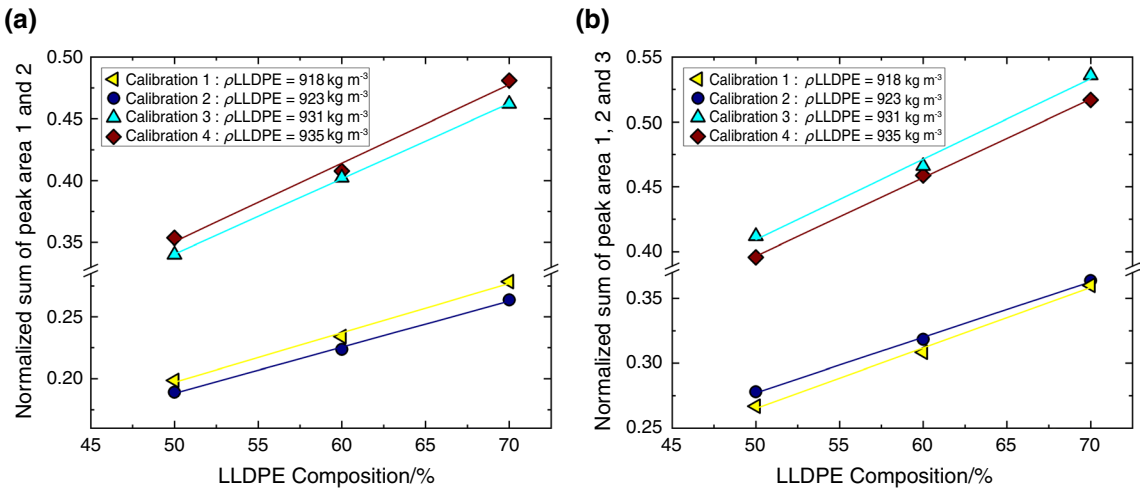

Fig. 5 Calibration curves obtained from the model DSC experimental curves considering (**A**) the first two peaks and (**B**) the first three peaks from the SSA fractionation melting curve

Table 4 Numerical results and correlation coefficient of the linear calibration curves based on SSA peak area determination

Calibration type	Calibration number	Slope	Intercept
Two peaks	Calibration 1	0.00399	−0.00259
	Calibration 2	0.00373	0.00182
	Calibration 3	0.00609	0.03618
	Calibration 4	0.00636	0.03275
Three peaks	Calibration 1	0.00466	0.03215
	Calibration 2	0.00428	0.06325
	Calibration 3	0.00605	0.09396
	Calibration 4	0.0062	0.09921

sequences, the analysis outcome with the normalized first two or three peaks will be a higher value in the calibration curves. Table 4 presents the fitting parameters derived from the calibration curves. We have chosen to compare the results obtained with both calibration curves (two and three peaks) to differentiate the effect of the co-crystallization over the estimation of LLDPE. As predicted, the calibration curves for the two peaks are less affected by co-crystallization with LDPE, thus representing the LLDPE content more closely.

Estimation of the composition of recycled blends

For the analysis of post-consumer polymer feedstocks, recognized for their heterogeneous composition and contamination [47, 48], the SSA methodology mentioned above was employed to estimate the LLDPE content. We investigated several post-consumer recyclate resins commercially marketed as blends of LLDPE and LDPE. Initially, the LDPE content was evaluated using a methodology previously developed by our group that utilizes a temperature-modulated DSC (TMDSC) [16]. For comparative purposes, the values obtained through this method were contrasted with those acquired using NMR. These values are presented in Table S3 in the supplementary information. A notable discrepancy was observed between the estimation from TMDSC and NMR in some materials. This can be attributed to the fact that recycled materials have a diverse composition, and the TMDSC method was initially designed for virgin materials. This may cause TMDSC to provide altered results when applied to recycled materials. For this reason, SSA is introduced as an alternative methodology. It aims to deliver precise results and offers a practical, cost-effective approach suitable for quality control assurance.

Within the context of this research, the LLDPE content in recycled materials was estimated using the previously established calibration curves (Fig. 5) obtained through the SSA methodology, considering the specific temperature range covering the first two and three peaks, which result from the last heating step in the SSA thermal protocol. For each recyclate material, the normalized sum of these peaks was determined. This value was then correlated with the respective calibration curve. This procedure was applied in each calibration curve, covering all density ranges. Refer to the supplementary information (Figure S8) for a more detailed calculation example in a specific recycled material.

Figure 6 compares the LLDPE composition determined from the calibration curves by the SSA methodology with the estimations derived from the NMR methodology. This comparison aims to evaluate the SSA efficacy against the results from the NMR, a known method for its robustness and precise prediction capabilities in polymer and recycled materials. The alignment of results from SSA with those of NMR highlights the potential of the former as a viable predictor of LLDPE composition. As observed in Fig. 6, the values obtained from the calibration curves agree with the NMR outcomes. Specifically, materials REC1 to REC5 display a good estimation, ideally approaching the diagonal dotted line, particularly in the 918–923 kg m^{-3} density range. However, when considering the estimations with the higher densities (Fig. 6C and D), one can notice that only the REC0 material from the SSA analysis is adjusted correctly. In addition, Figure S9 presents the results considering the calibration curves calculated with the first three peaks.

Considering the nature of the different recycled materials under investigation, which exhibit a complex molecular structure as presented in Fig. 7, they can also display different characteristics ranging from a high degree of branching distribution to very linear chain sequences. This diversity in molecular architecture makes the estimation process challenging, as it is impossible to establish a single calibration curve that accurately determines the specific composition of LDPE (low-density polyethylene)/LLDPE (linear low-density polyethylene). It is possible to note in Fig. 7 that the REC0 material presents an increased first peak with respect to the other fractions and also with respect to the other materials. This means that this material possesses more linear chains that are able to crystallize at higher temperatures instead of the broader distribution found in other recycled materials. In addition, to support this statement, CEF measurements of REC0 and REC3 showed a higher elution temperature for REC0 compared to REC3, confirming the structural differences in the chain distribution obtained in the SSA. Refer to the supplementary information in Figure S10.

We have formulated a qualitative parameter to establish the most appropriate calibration curve for an unknown recycled material. This is based on the understanding that recycled materials that contain longer uninterrupted chain fractions (i.e., higher densities or higher amounts of higher densities LLDPEs) will exhibit

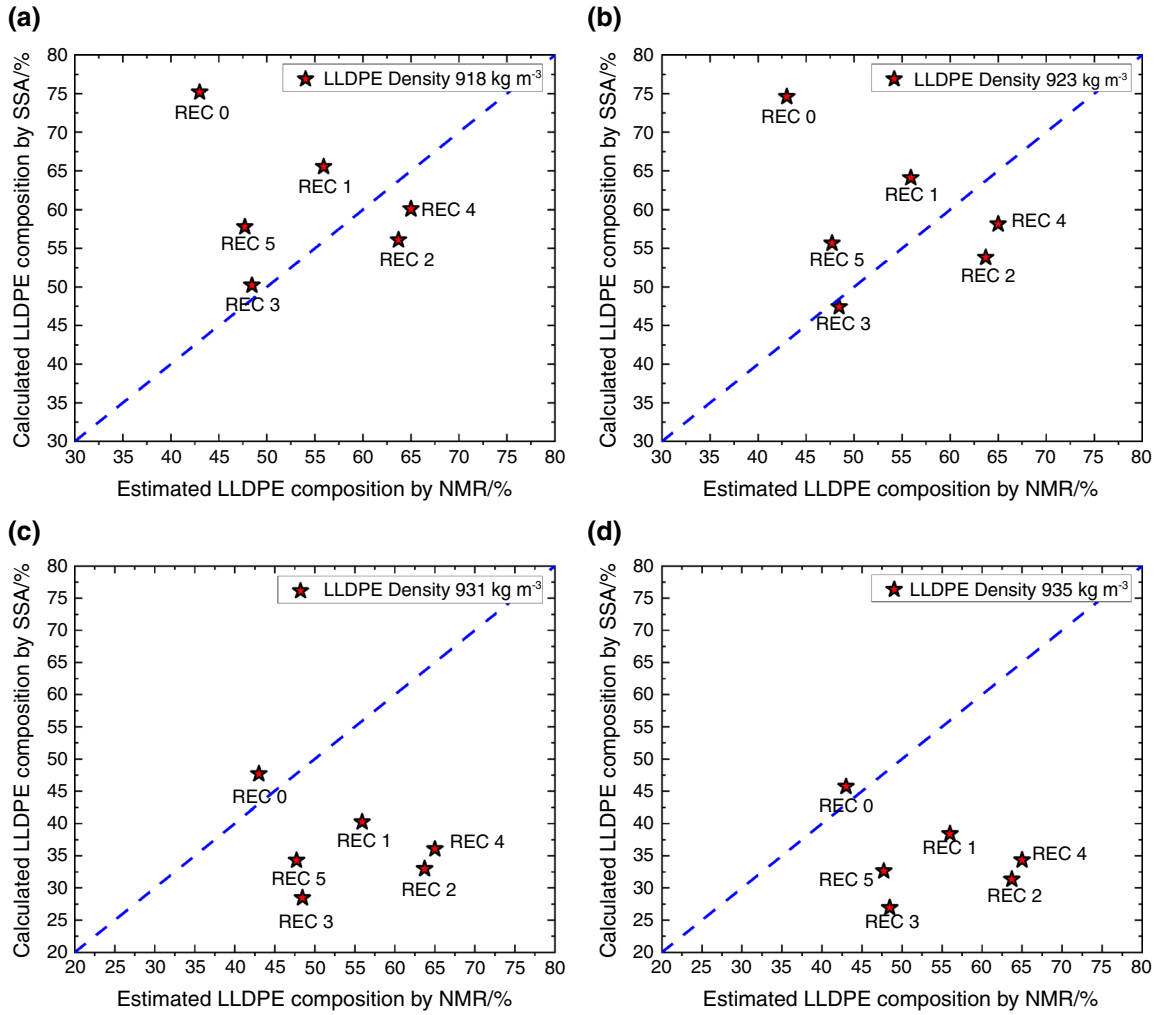

Fig. 6 Comparison of the estimated LLDPE composition by NMR and the calculated LLDPE composition by SSA of 6 different recycled materials, considering the first 2 areas of the fractionated melting SSA result at different LLDPE densities as (**A**) 918 kg m^{-3}; (**B**) 923 kg m^{-3}; (**C**) 931 kg m^{-3}; and (**D**) 935 kg m^{-3}

a more pronounced initial peak during the final heating phase as part of the successive self-nucleation and annealing (SSA) protocol. Given that these materials are more accurately quantified using calibration curves corresponding to higher densities, we propose the following criterion: If the area of the first peak is greater than 1.5 times that of the second peak, the material's composition is best determined using calibration curves designed for higher densities (931 and 935 kg m^{-3}).

In addition, if this condition is not met, calibration curves associated with lower densities (918 and 923 kg m^{-3}) should provide a more accurate estimation of the linear low-density polyethylene (LLDPE) content. This approach allows for a more tailored analysis of the polyethylene content, optimizing the accuracy of the compositional assessment.

where A_1 is the area under the first peak and A_2 is the area under the second peak. Using this methodology, it is possible to establish the composition of LLDPE in recycled post-consumer materials when considering the mentioned calibration curves. In addition, it is possible to integrate the protocol for estimating PP as contamination in the PCR. In this context, it is possible to estimate the approximate content of PP contamination, as presented in Table 2, and determine the content of LLDPE via one methodology.

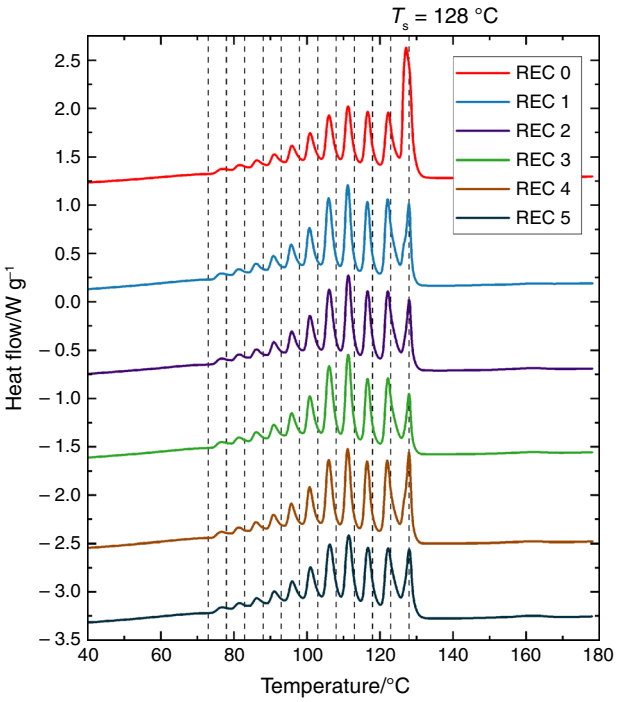

Fig. 7 Final DSC heating scan after applying the SSA protocol to the recycled materials using fractionation windows of 5 °C; the dashed vertical lines correspond to the employed values of T_s starting from T_s = 128 °C

Conclusions

This study presents a methodology based on the successive self-nucleation and annealing (SSA) technique for the qualitative analysis of post-consumer polymer feedstocks in the estimation of linear low-density polyethylene (LLDPE) and low-density polyethylene (LDPE) content within heterogeneous commercial recycled PE materials. This methodology offers an advantage over other methods that require more time and resources to be completed or provide an inadequate quantification. We have demonstrated that this approach quantifies LLDPE/LDPE ratio by consistently fractionating the constituent polymers in recycled materials.

Our findings indicate that traditional methods, such as temperature-modulated differential scanning calorimetry (TMDSC), may not provide accurate estimations when applied to recycled materials due to their varied composition compared to virgin blends. The proposed SSA methodology overcomes these limitations. Comparative analysis showed that the SSA protocol yields results that align more closely with those derived from nuclear magnetic resonance (NMR) measurements. This suggests that the SSA protocol could offer a more precise and practical alternative for the quality control assurance of recycled polymers.

Future work should focus on refining the SSA methodology for different types of polymer blends and exploring its applicability on an industrial scale. The ultimate goal is to enhance the sustainability of plastic recycling processes by providing reliable, cost-effective methods for material characterization.

Supplementary Information The online version contains supplementary material available at https://doi.org/10.1007/s10973-024-13199-0.

Acknowledgements This work has received funding from the European Union's Horizon 2020 research and innovation program under Grant Agreement No 860221 under the name of the REPOL project. AJM acknowledges funding from the Basque Government through grant IT1503-22.

Author's contribution SC-D helped in formal analysis, investigation, data curation, writing—original draft; AA contributed to writing—review & editing; DC was involved in writing—review & editing, supervision; DT helped in conceptualization, writing—review & editing, supervision; AJM contributed to conceptualization, writing—review & editing, supervision.

Funding Open Access funding provided thanks to the CRUE-CSIC agreement with Springer Nature.

References

1. Plastics Europe, Plastics - the Facts 2020 • Plastics Europe. Accessed: Jan. 03, 2022. [Online]. Available: https://plasticseurope.org/knowledge-hub/plastics-the-facts-2020/.
2. Andreasi Bassi S, Boldrin A, Faraca G, Astrup TF. Extended producer responsibility: How to unlock the environmental and economic potential of plastic packaging waste? Resour Conserv Recycl. 2020;162:105030. https://doi.org/10.1016/j.resconrec.2020.105030.
3. Bening CR, Pruess JT, Blum NU. Towards a circular plastics economy: Interacting barriers and contested solutions for flexible packaging recycling. J Clean Prod. 2021;302: 126966. https://doi.org/10.1016/j.jclepro.2021.126966.
4. Chen X, Kroell N, Wickel J, Feil A. Determining the composition of post-consumer flexible multilayer plastic packaging with near-infrared spectroscopy. Waste Manag. 2021;123:33–41. https://doi.org/10.1016/j.wasman.2021.01.015.
5. Alberghini M, et al. Sustainable polyethylene fabrics with engineered moisture transport for passive cooling. Nat Sustain. 2021. https://doi.org/10.1038/s41893-021-00688-5.
6. Zheng J, Arifuzzaman M, Tang X, Chelsea Chen X, Saito T. Recent development of end-of-life strategies for plastic in industry and academia: bridging their gap for future deployment. Mater

Horiz. 2023;10(5):1608–24. https://doi.org/10.1039/D2MH01549H.
7. Ragaert K, Delva L, Van Geem K. Mechanical and chemical recycling of solid plastic waste. Waste Manag. 2017;69:24–58. https://doi.org/10.1016/J.WASMAN.2017.07.044.
8. Lange J-P. Managing plastic waste─sorting, recycling, disposal, and product redesign. ACS Sustain Chem Eng. 2021;9(47):15722–38. https://doi.org/10.1021/acssuschemeng.1c05013.
9. Taylor J, Baik JJ. Benefits of coextruded LLDPE/LDPE film vs. blended LLDPE/LDPE film. J Plast Film Sheeting. 2000;16(3):223–36. https://doi.org/10.1106/1G5R-7BM4-1KB8-E7U4.
10. Mezghani K and Furquan SA, Lldpe-ldpe blown film blend, US20130245201A1, Sep. 19, 2013 Accessed: Jul. 31, 2023. [Online]. Available: https://patents.google.com/patent/US20130245201A1/en.
11. Spalding MA and Chatterjee AM, Handbook of industrial polyethylene and technology : definitive guide to manufacturing, properties, processing, applications and markets set., 1 online resource vols. Hoboken, NJ: Wiley, 2017. [Online]. Available: http://rbdigital.rbdigital.com.
12. Hashemnejad M. Composition analysis of post-consumer recycled blends of linear low- and low-density polyethylene using a solution-based technique. J Appl Polym Sci. 2023;140(30): e54099. https://doi.org/10.1002/app.54099.
13. Mavridis H, High clarity polyethylene films, US9029478B2, May 12, 2015 Accessed: Aug. 01, 2023. [Online]. Available: https://patents.google.com/patent/US9029478B2/en.
14. Lohse DJ, et al. Well-defined, model long chain branched polyethylene. 2. Melt rheological behavior. Macromolecules. 2002;35(8):3066–75. https://doi.org/10.1021/ma0117559.
15. Cecon VS, Da Silva PF, Vorst KL, Curtzwiler GW. The effect of post-consumer recycled polyethylene (PCRPE) on the properties of polyethylene blends of different densities. Polym Degrad Stab. 2021;190: 109627. https://doi.org/10.1016/j.polymdegradstab.2021.109627.
16. Scoppio A, Cavallo D, Müller AJ, Tranchida D. Temperature modulated DSC for composition analysis of recycled polyolefin blends. Polym Test. 2022;113: 107656. https://doi.org/10.1016/j.polymertesting.2022.107656.
17. Juan R, Paredes B, García-Muñoz RA, Domínguez C. Quantification of PP contamination in recycled PE by TREF analysis for improved the quality and circularity of plastics. Polym Test. 2021;100: 107273. https://doi.org/10.1016/j.polymertesting.2021.107273.
18. Prasad A. A quantitative analysis of low density polyethylene and linear low density polyethylene blends by differential scanning calorimetery and fourier transform infrared spectroscopy methods. Polym Eng Sci. 1998;38(10):1716–28. https://doi.org/10.1002/pen.10342.
19. Góra M, Tranchida D, Albrecht A, Müller AJ, Cavallo D. Fast successive self-nucleation and annealing (SSA) thermal fractionation protocol for the characterization of polyolefin blends from mechanical recycling. J Polym Sci. 2022;60(24):3366–78. https://doi.org/10.1002/pol.20220104.
20. Lee HS, Denn MM. Blends of linear and branched polyethylenes. Polym Eng Sci. 2000;40(5):1132–42. https://doi.org/10.1002/pen.11241.
21. Monwar M, Yu Y. Determination of the composition of LDPE/LLDPE blends via 13C NMR. Macromol Symp. 2020;390(1):1900013. https://doi.org/10.1002/masy.201900013.
22. Fillon B, Wittmann JC, Lotz B, Thierry A. Self-nucleation and recrystallization of isotactic polypropylene (α phase) investigated by differential scanning calorimetry. J Polym Sci Part B Polym Phys. 1993;31(10):1383–93. https://doi.org/10.1002/POLB.1993.090311013.
23. Michell RM, Mugica A, Zubitur M, Muller AJ. Self-nucleation of crystalline phases within homopolymers, polymer blends, copolymers, and nanocomposites. Adv Polym Sci. 2015;276:215–56. https://doi.org/10.1007/12_2015_327.
24. Sangroniz L, Cavallo D, Müller AJ. Self-nucleation effects on polymer crystallization. Macromolecules. 2020;53(12):4581–604. https://doi.org/10.1021/acs.macromol.0c00223.
25. Müller AJ, Arnal ML. Thermal fractionation of polymers. Prog Polym Sci. 2005;30(5):559–603. https://doi.org/10.1016/j.progpolymsci.2005.03.001.
26. Müller AJ, Michell RM, Pérez RA, Lorenzo AT. Successive self-nucleation and annealing (SSA): correct design of thermal protocol and applications. Eur Polym J. 2015;65:132–54. https://doi.org/10.1016/j.eurpolymj.2015.01.015.
27. Carmeli E, Tranchida D, Albrecht A, Müller AJ, Cavallo D. A tailor-made successive self-nucleation and annealing protocol for the characterization of recycled polyolefin blends. Polymer. 2020;203: 122791. https://doi.org/10.1016/J.POLYMER.2020.122791.
28. Coba-Daza S, et al. Effect of compatibilizer addition on the surface nucleation of dispersed polyethylene droplets in a self-nucleated polypropylene matrix. Polymer. 2022;263: 125511. https://doi.org/10.1016/j.polymer.2022.125511.
29. Müller AJ, Hernández ZH, Arnal ML, Sánchez JJ. Successive self-nucleation/annealing (SSA): a novel technique to study molecular segregation during crystallization. Polym Bull. 1997;39(4):465–72. https://doi.org/10.1007/s002890050174.
30. Müller AJ, Lorenzo AT, Arnal ML. Recent advances and applications of 'successive self-nucleation and annealing' (SSA) high speed thermal fractionation. Macromol Symp. 2009;277(1):207–14. https://doi.org/10.1002/masy.200950325.
31. Kong Y, Hay JN. The enthalpy of fusion and degree of crystallinity of polymers as measured by DSC. Eur Polym J. 2003;39(8):1721–7. https://doi.org/10.1016/S0014-3057(03)00054-5.
32. Schick C. Differential scanning calorimetry (DSC) of semicrystalline polymers. Anal Bioanal Chem. 2009;395(6):1589–611. https://doi.org/10.1007/s00216-009-3169-y.
33. Larsen ÅG, Olafsen K, Alcock B. Determining the PE fraction in recycled PP. Polym Test. 2021;96: 107058. https://doi.org/10.1016/j.polymertesting.2021.107058.
34. Workman JJ. Quantification of LDPE [Low Density Poly(Ethylene)], Lldpe [Linear Low Density Poly(Ethylene)], and Hdpe [High Density Poly(Ethylene)] in polymer film mixtures 'as received' using multivariate modeling with data augmentation (data fusion) and infrared, Raman, and near-infrared spectroscopy. Spectrosc Lett. 1999;32(6):1057–71. https://doi.org/10.1080/00387019909350050.
35. Manivannan A and Seehra MS, Identification and quantification of polymers in waste plastics using differential scanning calorimetry, In: Preprints of Symposia-Division of Fuel Chemistry American Chemical Society, 1997, pp. 1028–1032.
36. Pasch H, Brüll R, Wahner U, Monrabal B. Analysis of polyolefin blends by crystallization analysis fractionation. Macromol Mater Eng. 2000;279(1):46–51. https://doi.org/10.1002/1439-2054(20000601)279:1%3c46::AID-MAME46%3e3.0.CO;2-1.
37. Olabisi O and Adewale K, Handbook of Thermoplastics. in Plastics Engineering. CRC Press, 2016. [Online]. Available: https://books.google.es/books?id=kjg0CwAAQBAJ.
38. Utracki LA, Mukhopadhyay P, Gupta RK. Polymer blends: introduction. In: Utracki LA, Wilkie CA, editors. Polymer blends handbook. Dordrecht: Springer, Netherlands; 2014. p. 3–170.
39. Utracki LA. Polyethylenes and Their Blends. In: Utracki LA, Wilkie CA, editors. Polymer Blends Handbook. Dordrecht: Springer, Netherlands; 2014. p. 1559–732.

40. Roosen M, et al. Expanding the collection portfolio of plastic packaging: impact on quantity and quality of sorted plastic waste fractions. Resour Conserv Recycl. 2022;178: 106025. https://doi.org/10.1016/j.resconrec.2021.106025.
41. Wagner J, Phillips PJ. The mechanism of crystallization of linear polyethylene, and its copolymers with octene, over a wide range of supercoolings. Polymer. 2001;42(21):8999–9013. https://doi.org/10.1016/S0032-3861(01)00386-X.
42. Carmeli E, Fenni SE, Caputo MR, Müller AJ, Tranchida D, Cavallo D. Surface nucleation of dispersed polyethylene droplets in immiscible blends revealed by polypropylene matrix self-nucleation. Macromolecules. 2021;54(19):9100–12. https://doi.org/10.1021/acs.macromol.1c01430.
43. Góra M, et al. Surface-enhanced nucleation in immiscible polypropylene and polyethylene blends: the effect of polyethylene chain regularity. Polymer. 2023;282: 126180. https://doi.org/10.1016/j.polymer.2023.126180.
44. Wang W, et al. Surface nucleation of dispersed droplets in double semicrystalline immiscible blends with different matrices. Macromol Chem Phys. 2022;223(21):2200202. https://doi.org/10.1002/macp.202200202.
45. Fenni SE, Caputo MR, Müller AJ, Cavallo D. Surface roughness enhances self-nucleation of high-density polyethylene droplets dispersed within immiscible blends. Macromolecules. 2022;55(4):1412–23. https://doi.org/10.1021/acs.macromol.1c02487.
46. Drummond KM, Hopewell JL, Shanks RA. Crystallization of low-density polyethylene- and linear low-density polyethylene-rich blends. J Appl Polym Sci. 2000;78(5):1009–16. https://doi.org/10.1002/1097-4628(20001031)78:5%3c1009::AID-APP100%3e3.0.CO;2-2.
47. Belyamani I, et al. Toward recycling ″unsortable″ post-consumer WEEE stream: characterization and impact of electron beam irradiation on mechanical properties. J Clean Prod. 2021;294: 126300. https://doi.org/10.1016/j.jclepro.2021.126300.
48. Curtzwiler GW, Schweitzer M, Li Y, Jiang S, Vorst KL. Mixed post-consumer recycled polyolefins as a property tuning material for virgin polypropylene. J Clean Prod. 2019;239: 117978. https://doi.org/10.1016/j.jclepro.2019.117978.